

TECHNISCHE HOGESCHOOL
VLIEGTUIGBOUWKUNDE
KANAALSTRAAT 10 - DELFT
HOLLAND

groep: *Stabiliterekening*
prijs: *11.-*
d.d.: 11 DEC. 1953
paraf: *Maxel Ambe*

The local instability of compression members
built up from flat plates,
by
Prof. dr ir A. van der Neut

Report V.T.H. - 47

TECHNISCHE HOGESCHOOL
SUB-AFD. VLIEGTUIGBOUWKUNDE

RAPPORT VTH - 47

THE LOCAL INSTABILITY OF COMPRESSION MEMBERS,
BUILT UP FROM FLAT PLATES

by :

Prof. Dr. Ir. A van der Neut

Dit onderzoek is uitgevoerd met steun
van het Delfts Hogeschoolfonds.

DELFT

August 1952

The local instability of compression members, built up from flat plates.

by Prof. Dr Ir A. van der Neut.

Summary

The problem of local instability of structures, composed of flat plates, rigidly connected along the longitudinal edges, is essentially to find the interaction between the composing plates, resulting in equality of buckling stresses and wave lengths for all individual plates. With complicated structures, like plates reinforced by longitudinal stiffeners, the computations required for determining the exact solution are highly laborious. This paper presents an exact method, which reduces the amount of numerical work by applying nomograms, giving the relation between buckling stress, wave length and edge restraint. The method can be applied to structures composed of an arbitrary number of walls (section 4 and 5). Explicit formulae have been given for structures with 4 or less joints connecting the walls (section 7). The procedure is illustrated by a numerical example.

Contents

1. Introduction
2. Assumptions
3. Buckling of a web with edge restraint
4. Buckling of an arbitrary sequence of plates
5. Extension to closed and bifurcating sections
6. The coefficients of restraint
7. Applications
8. Numerical Example
9. Notations
10. References

Acknowledgements.

1. Introduction

Semi-monocoque structures, as applied in aircraft and in some types of ships, consist of sheet, reinforced by regularly spaced longitudinal stiffeners supported by frames. When loaded in longitudinal compression failure by instability occurs. According to the type of buckling deformation the instability may be classified as: 1. column failure; 2. torsional instability; 3. general instability; 4. local instability.

With column failure or Euler instability all stiffeners are bending in the direction normal to the sheet, the frames behaving as rigid supports. With torsional instability the cross section of the stiffeners rotates in the plane normal to the longitudinal axis of the stiffeners, except the cross sections located in the plane of the frames. General instability may occur when frames are relatively weak in bending. The frames will buckle together with the stiffeners; the half wave length comprising more than one frame distance.

Whereas the wave length with the first two types of buckling is governed by frame spacing, with local instability the wave length is much smaller than the frame distance and it is practically independent of conditions presented by the frames. Moreover in contrast to the former types the cross section of the stiffeners can no longer be considered to remain undistorted in its plane. Any of the composing walls of the stiffeners as well as the sheet panels buckle in the manner of plates loaded in compression, the half wave length being of the order of magnitude of the width of the individual plates.

The coherence of the individual plates however requires that the wave patterns of different individual plates are compatible. Therefore the problem of computing the local buckling load is how to apply plate theory such that the interaction of collaborating plates is accounted for adequately. Commonly used engineering methods for determining the local buckling stress of stiffeners consider each individual plate to have hinge support at the line of intersection with the adjacent walls. The buckling stress is assumed to be equal to the weighted average of the, in general unequal, buckling stresses of the composing plates. (ref.1). This approach is unsatisfactory in many respects; though for rapid determination of a first approximation it proves to be quite useful. It does not present compatible wave patterns since wave lengths of the individual walls are unequal; hinge support is being assumed, whereas in fact the longitudinal edges of the plates are restraint elastically by the adjoining plates; the buckling stresses computed for the individual plates are unequal, whereas in fact interaction equalizes these buckling stresses. The reliability of this method

decreases when the interaction is more important due to increasing difference in the width to thickness ratio (b/t) of individual plates. Such conditions occur with stiffened sheet, where b/t of sheet panels is much larger than that of stiffener walls. For this case a more rigid analysis is required, accounting for the interaction. This applies more in particular to modern aircraft wings, where the compressive load per unit of width is very high, due to the large size of the aircraft or the small thickness of the wing. Whereas formerly it was tolerated that skin panels buckled at loads far below the ultimate load, aerodynamic cleanness and weight economy may require nowadays that the skin does not buckle and remains fully effective up to the ultimate load. This means that the local buckling stress of the skin-stiffener combination should preferably be equal to the buckling stress with respect to column failure or torsionnal instability. Consequently aeronautical engineering needs a straightforward approach to the local instability problem.

The derivation of the stability criterium for a structure composed of a sequence of rectangular plates does not present fundamental difficulties. The fourth order differential equation yielding for each composing plate 4 integration constants the determinant is of the order equal to 4 times the number of composing plates. However the numerical work required for evaluating the determinant is quite laborious. In this way the local buckling stresses for stiffeners having Z- and channel section have been computed (ref.2).

In the same manner the problem has been solved for panels stiffened by top-hat section stringers, neglecting however the stringer flanges (ref. 3).

The object of this paper is to present a more straightforward method, enabling the solution for quite complicated systems with a relatively small amount of computational work; this latter being cut down by applying a set of nomograms presented in this paper.

2. Assumptions

The structure considered in this paper is composed out of flat plates; each plate having constant thickness and constant width. So it comprises flat panels, stiffened by Z-, channel and square tophat section stiffeners, but it does not include either rounded tophat stiffeners or stiffeners with flange edges reinforced by bulbs or lips.

The method developed in this paper has been based upon the following assumptions:

- 1) The wave length being a small multiple of the lateral dimensions of

the stiffeners the shear loads and bending moments in the plane of each individual wall will remain small; consequently the strains in the centre of the plate thickness are negligably small and the displacements of the centre in the plane of the plate can be neglected. Hence the line of intersection of the centre planes of two successive walls is considered to have no displacement at all: each composing plate will be assumed to have at its edges rigid support, except plates with free edges. Plates with 2 supported edges will be called webs; plates with one supported edge and one free edge flanges. Flange edge reinforcements, even if they are of constant thickness, cannot be considered to have no displacements in the plane normal to the flange, since the width of the edge reinforcement is small compared to the wave length. As long as an extension of this theory covering reinforced flanges is missing, a conservative estimate of the critical load is obtained by neglecting the effect of the reinforcement.

- 2) The flexibility of the corner between two adjoining walls is neglected. Hence the rotations of coinciding edges of two adjoining plates are assumed to be equal.
- 3) The wave length is independent of frame spacing and that magnitude of wave length is assumed which makes the local buckling stress minimal. Likewise the influence of the conditions at the loaded edges can be neglected, i.e. the panel can be considered to have infinite length.
- 4) With riveted structures the joint between the sheet and the flanges of the stiffeners is situated near the middle of the flange. However it will be assumed that the joint is situated at the corner between flange and web of the stiffener, so as to obtain a sheet panel with supported edges. As far as the sheet panel is concerned this assumption does not influence its condition of loading very much; however the loads on the flange will differ rather importantly in the assumed scheme and the actual structure. Due to the fact that the cross section of these flanges is small compared to the total cross section it may be expected that this assumption does not influence the critical load of the whole panel importantly.
- 5) Hooke's law is being assumed throughout, though a further development proves to be possible covering the plastic range.

3. Buckling of a web with edge restraint.

The differential equation of a flat plate loaded in longitudinal compression is

$$D \Delta^2 w = - \frac{t}{B} \sigma \frac{\partial^2 w}{\partial x^2} \quad (3-1)$$

With elastic restraint against rotation at the rigidly supported

edges the boundary conditions are (see fig.1):

$$y = -\frac{1}{2}b : w = 0, \quad M_1 = B \frac{\partial^2 w}{\partial y^2} = +C_1 \left(\frac{B}{b}\right) \varphi_1 \quad (3-2a)$$

$$y = \frac{1}{2}b : w = 0, \quad M_2 = B \frac{\partial^2 w}{\partial y^2} = -C_2 \left(\frac{B}{b}\right) \varphi_2 \quad (3-2b)$$

where C_1, C_2 are coefficients, expressing the stiffness of restraint. The general solution of (1) for an infinitely long plate is.

$$w = (A_1 \cosh \alpha y + A_2 \cos \beta y + A_3 \sinh \alpha y + A_4 \sin \beta y) \sin \frac{\pi x}{l}$$

This solution is composed out of a symmetrical part and an anti-symmetrical part. Hence, for an arbitrary set of edge restraints C_1, C_2 the buckling mode can be decomposed into a symmetrical and an anti-symmetrical buckling mode w_s and w_a resp. Both modes occurring at the same buckling stress, the stiffness of edge restraint, equal at both edges, must be such in both cases that the buckling stresses are equal for equal wave length $2l$.

The boundary conditions replacing (2a,b) are (see fig.2)

$$y = \frac{1}{2}b : w_s = 0, \quad M_s = B \frac{\partial^2 w_s}{\partial y^2} = -C_s \frac{B}{b} \varphi_s$$

$$y = \frac{1}{2}b : w_a = 0, \quad M_a = B \frac{\partial^2 w_a}{\partial y^2} = -C_a \frac{B}{b} \varphi_a$$

The identity $w = w_a + w_s$ yields (compare fig.1 and 2)

$$M_1 = -M_a + M_s,$$

$$M_2 = M_a + M_s \quad \text{or}$$

$$C_1 \frac{B}{b} (\varphi_a - \varphi_s) = \frac{B}{b} (C_a \varphi_a - C_s \varphi_s) \quad (3-3a)$$

$$-C_2 \frac{B}{b} (\varphi_a + \varphi_s) = -\frac{B}{b} (C_a \varphi_a + C_s \varphi_s) \quad (3-3b)$$

For a given set of stiffnesses C_1 and C_2 , the equations (3a,b) together with the condition that the buckling stresses for the symmetrical and the antisymmetrical case are equal, define the stiffnesses C_a, C_s and the ratio φ_a/φ_s . Thus the possibility of the decomposition of the general case with unequal stiffnesses C_1, C_2 into a symmetrical and an antisymmetrical case has been shown.

4. Buckling of an arbitrary sequence of plates

There are n plates numbered successively $1, 2, \dots, i, \dots, n$.

The rotation of the edge of plate i , forming the joint with plate $i - 1$ is denoted by $\varphi_{i, i-1}$; the rotation of the other edge of plate i is $\varphi_{i, i+1}$.

These rotations are positive in the anti-clockwise direction. According to assumption (2)

$$\varphi_{i-1, i} = \varphi_{i, i-1} \quad (4-1)$$

$$\varphi_{i, i+1} = \varphi_{i+1, i}$$

Decomposing the rotations into a symmetrical and an anti-symmetrical part (compare fig.2) it follows

$$\varphi_{i, i-1} = \varphi_{a, i} - \varphi_{s, i} \quad (4-2)$$

$$\varphi_{i, i+1} = \varphi_{a, i} + \varphi_{s, i}$$

The edges of the plate i are loaded by the elastic restraining moments $M_{i, i-1}$ and $M_{i, i+1}$, using the same denotation and positive direction as for φ_i . Applying the decomposition into symmetrical and anti-symmetrical part, follows:

$$M_{i, i-1} = M_{a, i} - M_{s, i} \quad (4-3)$$

$$M_{i, i+1} = M_{a, i} + M_{s, i}$$

where

$$M_a = -\frac{B}{b} c_a \varphi_a \quad (4-4)$$

$$M_s = -\frac{B}{b} c_s \varphi_s$$

The condition of equilibrium of the joint $i-1, i$ requires

$$M_{i-1, i} + M_{i, i-1} = 0 \quad (4-5)$$

Substituting (2) into (1) and (3), (4) into (5) yields

$$(\varphi_a + \varphi_s)_{i-1} = (\varphi_a - \varphi_s)_i \quad (4-6)$$

$$-\left[\frac{B}{b}(c_a \varphi_a + c_s \varphi_s)\right]_{i-1} - \left[\frac{B}{b}(c_a \varphi_a - c_s \varphi_s)\right]_i = 0 \quad (4-7)$$

For a given stress σ and half wave length l the coefficients of restraint c_a and c_s , which are required for equilibrium can be computed (see sect.6). Therefore they may be considered to be known quantities. Then, when $\varphi_{a, i-1}, \varphi_{s, i-1}$ are known, the rotations $\varphi_{a, i}, \varphi_{s, i}$ can be solved from the equations (6), (7). Applying (6), (7) to the next joint $i, i+1$, $\varphi_{a, i+1}, \varphi_{s, i+1}$ can be solved, etc. So these equations are recurrent equations enabling the computation of the whole buckling mode as soon as for one of the composing plates the decomposition into φ_a and φ_s is known. Usually more possibilities exist for starting the solution of the

recurrent equations:

1. Usually it

may be that the cross section of the composed structure is regular in such a way that a plane of symmetry or anti-symmetry of the mode can be indicated. For instance in the case of a channel section, the critical mode will be symmetrical. Denoting the middle wall with index 1, it is known that $\varphi_{a1} = 0$. For φ_{s1} , an arbitrary value can be chosen, since the magnitude of the deformation is indefinite in buckling problems.

2. When the cross section is open, the outmost walls will be flanges with one free edge, the other edge being supported and elastically restrained. The behaviour of the flange depends upon a single coefficient of restraint C . Denoting one of the end flanges with index 1, the relation between restraining moment and edge rotation is

$$M_{1,2} = -\left(\frac{B}{6}C\right)\varphi_{1,2}$$

Then the equations (6), (7) have to be replaced for $i = 2$ by

$$\varphi_{1,2} = (\varphi_a - \varphi_s)_2 \quad ; \quad -\left(\frac{B}{6}C\right)\varphi_{1,2} - \left[\frac{B}{6}(C_a\varphi_a - C_s\varphi_s)\right]_2 = 0 \quad (4-8,9)$$

Taking for $\varphi_{1,2}$ an arbitrary value, $\varphi_{a2}, \varphi_{s2}$ can be computed from (8), (9) and the recurrent equations (6), (7) for $i = 3, 4, \dots, n-1$ can be solved.

The fact, that an arbitrary combination of values for σ and λ has been chosen for solving the recurrent equations, in general means that in addition to the longitudinal compression or other external loads must be applied for equilibrium. Only when σ is equal to the buckling stress σ_b corresponding to the assumed half wave length λ these external loads are zero.

The need for external load appears at the last joint, between the walls $n-1$ and n , where equilibrium requires the external moment $m_{n-1,n}$. The condition of equilibrium of this joint is

$$m_{n-1,n} - M_{n-1,n} - M_{n,n-1} = 0 \quad (4-10)$$

$M_{n,n-1}$ depends upon $\varphi_{n,n-1}$ only, since wall n is the last wall of the sequence. Therefore $(\varphi_a)_{n-1}, (\varphi_s)_{n-1}$ is the final set of unknown quantities occurring in the recurrent equations, and $M_{n-1,n} + M_{n,n-1}$ does not vanish in general; for equilibrium the moment $m_{n-1,n}$ has to be added. This moment can be realized by a spring of stiffness

$R_{n-1,n} = -(m/\varphi)_{n-1,n}$, restraining the joint against rotation. When

$R_{n-1,n} > 0$ equilibrium requires an addition of stiffness; this means that without this added stiffness the structure is unstable and that the buckling stress σ_b at the assumed value of λ is smaller than σ . When $R_{n-1,n} < 0$ equilibrium requires a reduction of stiffness, which may mean that the actual structure is stable and that the buckling stress σ_b at the assumed value of λ is larger than σ . However this statement does not hold in general; it appears from the numerical example given in fig. 10 that $R < 0$ may occur for $\sigma < \sigma_b$. In such a case the transit-

ion between the ranges of negative and positive R is formed by the asymptotic value $R = \pm \infty$ following from $\varphi_{n-1,n} = 0$. Therefore the conclusion from $R < 0$ that $\sigma_b > \sigma$ should be taken with some caution. Nevertheless the sign of R helps to guide the choice of σ .

Computing $R_{n,n-1}$ for an assumed value of l and some values of σ , σ_b for the half wave length l can be determined graphically by interpolation (fig.3). Repeating these computations for other values of l the relation between l and σ_b is obtained, from which the critical stress and the corresponding wave length can be determined (fig.4).

The expression for $R_{n-1,n}$ depends upon the character of wall n .

Both cases considered for wall 1 will be considered here for wall n .

1. If wall n is supported along both its edges and its deformation has to be symmetrical: $\varphi_{an} = 0$; $\varphi_{sn} = (\varphi_a + \varphi_s)_{n-1}$

$$M_{n,n-1} = - \left(\frac{B}{b} C_s \right)_n (\varphi_a + \varphi_s)_{n-1}$$

Then (4.10) yields:

$$R_{n-1,n} = \left[\frac{B}{b} \frac{C_a \varphi_a + C_s \varphi_s}{\varphi_a + \varphi_s} \right]_{n-1} + \left(\frac{B}{b} C_s \right)_n \quad (4-10a)$$

2. If wall n is a flange

$$M_{n,n-1} = - \left(\frac{B}{b} C \right)_n (\varphi_a + \varphi_s)_{n-1}$$

hence

$$R_{n-1,n} = \left[\frac{B}{b} \frac{C_a \varphi_a + C_s \varphi_s}{\varphi_a + \varphi_s} \right]_{n-1} + \left(\frac{B}{b} C \right)_n \quad (4-10b)$$

The procedure outlined above enables a straightforward determination of σ_{crit} provided the coefficients of restraint C_a , C_s and C are available as functions of σ and l . Nomograms for the determination of these coefficients have been given in section 6.

5. Extension to closed and bifurcating sections

In section 4 it has been assumed that the sequence of plates forms a structure with open cross section. Some supplementary remarks are concerned with the case that the structure forms a closed section.

Next the case will be considered that more than 2 walls are joining forming a bifurcating joint.

5.1 Closed crossed section

When the cross section is symmetrical the problem reduces to the problem for the open section, limited by the plane of symmetry. When symmetry is not available the solution is obtained by superposition of 2 buckling modes (I and II) with arbitrary edge rotations of wall 1.

Solution I starts with $\varphi_{a1} = 0$, $\varphi_{s1} = 1$ and yields $(\varphi_{an})_I$,

$(\varphi_{sn})_I$

Solution II starts with $\varphi_{a1} = 1$; $\varphi_{s1} = 0$;

and yields $(\varphi_{an})_{II}$, $(\varphi_{sn})_{II}$

The superposition $\varphi = \varphi_I + X \varphi_{II}$ yields

$$\varphi_{1,n} = \varphi_{a1} - \varphi_{s1} = X - 1$$

$$\varphi_{n,1} = \varphi_{an} + \varphi_{sn} = (\varphi_{an} + \varphi_{sn})_I + X(\varphi_{an} + \varphi_{sn})_{II}$$

Then, $\varphi_{1,n} = \varphi_{n,1}$ guaranteeing the continuity at the joint n,1, yields:

$$X = \frac{1 + (\varphi_{an} + \varphi_{sn})_{II}}{1 - (\varphi_{an} + \varphi_{sn})_{II}}$$

Applying (10) to the joint n,1 the moment $m_{n,1}$ required to obtain equilibrium, is obtained.

5.2 Bifurcating cross section

In stiffened panels bifurcations are always present. The solution is obtained along the principles given in section 4, equating the rotations of all walls meeting in the point of bifurcation and requiring the equilibrium of moments acting upon the joint.

The procedure will be illustrated by 2 examples: a panel stiffened by top-hat section stiffeners and a panel stiffened by Z-stiffeners, alternating in size.

Panel with tophat stiffeners (fig.5)

Due to the symmetry of the continuous structure the critical mode will be symmetrical with respect to the planes of symmetry A en B. This observation overcomes the complication imposed by the occurrence of closed sections.

The continuous sequence of main walls is 1, 2, 3. The supplementary walls 1', 1'', introducing the bifurcation at joint 1,2, are added to this sequence; they obtain the lower figure of those of both main walls, since the moments exerted by these supplementary walls depend upon the rotation of joint 1,2 only.

Symmetry with respect to A and B resp. yields.

$$\varphi_{a1} = 0 \quad ; \quad \varphi_{a1'} = 0$$

Hence

$$\varphi_{12} = \varphi_{s1} = \varphi_{s1'} = \varphi_{1''2} = \varphi_{a2} - \varphi_{s2} \quad (5-1)$$

The condition of equilibrium of joint 1,2 is

$$M_{12} + M_{1'2} + M_{1''2} + M_{21} = 0 \quad (5-2)$$

Expressing the moments in the rotations it follows

$$-\left[\left(\frac{B}{b} c_s\right)_1 + \left(\frac{B}{b} c_s\right)_{1'} + \left(\frac{B}{b} c\right)_{1''}\right] \varphi_{s1} - \left[\frac{B}{b} (c_a \varphi_a - c_s \varphi_s)\right]_2 = 0 \quad (5-3)$$

From (1) and (2) φ_{2a} , φ_{2s} can be computed.

Due to symmetry with respect to B, $\varphi_{a2} = 0$.

Then the additional restraint at joint 2,3 is given by (4.10a), where $n = 3$.

Panel with alternating Z-stiffeners (fig.6)

The planes A and B are planes of symmetry for the structure, since with this problem the direction of the flanges is not essential. The structure might be replaced by that given in fig.7.

The critical mode will be anti-symmetrical with respect to the planes A en B.

The continuous sequence of main walls is as indicated in fig.6; n being 5. The supplementary walls 2' and 3'' have obtained their figure by the same reasoning as given in the former example. The walls 3' and 3'' have obtained their figure in view of the fact that their edge moments can be derived from those of wall 3.

The equations for joint 1,2 are (4.8), (4.9), yielding $\varphi_{a2}, \varphi_{s2}$. Equality of rotations at joint 2,3 yields.

$$\varphi_{a2} + \varphi_{s2} = \varphi_{2'3} = \varphi_{a3} - \varphi_{s3} \quad (5-4)$$

The condition of equilibrium of joint 2,3 is

$$M_{2,3} + M_{2'3} + M_{3,2} + M_{3'2} = 0$$

Due to antisymmetry. $M_{3'2} = M_{3,2}$. Expressing the moments in the rotations it follows.

$$-\left(\frac{B}{b}\right)_2 (c_a \varphi_a + c_s \varphi_s)_2 - \left(\frac{B}{b} c\right)_2 (\varphi_a + \varphi_s)_2 - 2\left(\frac{B}{b}\right)_3 (c_a \varphi_a - c_s \varphi_s)_3 = 0 \quad (5-5)$$

From (4) and (5) $\varphi_{a3}, \varphi_{s3}$ can be computed.

In the same way the joint 3,4 can be considered:

$$\varphi_{a3} + \varphi_{s3} = \varphi_{a4} - \varphi_{s4} \quad (5-6)$$

$$-2\left(\frac{B}{b}\right)_3 (c_a \varphi_a + c_s \varphi_s)_3 - \left(\frac{B}{b} c\right)_3 (\varphi_a + \varphi_s)_3 - \left(\frac{B}{b}\right)_4 (c_a \varphi_a - c_s \varphi_s)_4 = 0 \quad (5-7)$$

yielding $\varphi_{a4}, \varphi_{s4}$.

The additional restraint required at joint 4,5 is given by (4.10 b) where $n = 5$.

6. The coefficients of restraint

6.1 The nomograms of c_s , c_a and c .

The application of the method given in sec. 4 requires knowledge of the coefficients of restraint as functions of σ and l for 3 cases:

1. symmetric buckling of a web (c_s);
2. anti-symmetric buckling of a web (c_a);
3. buckling of a flange (c).

The buckling stress of a plate can be expressed by a coefficient k defined by

$$\sigma = k^2 \frac{\pi^2 B}{b^2 t}$$

and the half wave length l can be replaced by the coefficient λ defined by

$$l = \frac{1}{\lambda} \pi b$$

Then C_s , C_a and C are to be given as functions of k and λ . The exact solutions for these elementary stability problems is (ref.4).

$$C_s = - \frac{p^2 + q^2}{p \operatorname{tgh} p + q \operatorname{tg} q} \quad C_a = - \frac{p^2 + q^2}{p \operatorname{ctgh} p - q \operatorname{ctg} q} \quad (6-1,2)$$

where

$$\frac{p}{q} = \frac{1}{2} \left[\pm \lambda^2 + \pi k \lambda \right]^{\frac{1}{2}}$$

and

$$C = - \frac{(p^2 + q^2) (P^2 q \sinh p \cos q - Q^2 p \cosh p \sin q)}{(P^2 + Q^2) p q \cosh p \cos q + 2 P Q p q + (P^2 q^2 - Q^2 p^2) \sinh p \sin q} \quad (6-4)$$

where

$$\frac{p}{q} = \left[\pm \lambda^2 + \pi k \lambda \right]^{\frac{1}{2}}$$

When applying the method of sec.4 a large number of coefficients of restraint has to be determined. The computation has to be carried out for 3 or 4 values of the stress, and 3 or 4 wavelengths. For every wall 1 or 2 coefficients of restraint have to be determined with any set σ , l . Hence for a structure composed of m walls m (1 to 2) (9 to 16) coefficients have to be computed. This requires readily applicable information on C_s , C_a and C .

Graphs from which C_s and C as functions of k and λ can be taken, have been given in ref. 4a and b. However these graphs are confined to positive values of C_s and C , whereas the restraint in composed structures may be negative. Moreover application of these graphs is tedious, since the graphs contain only a limited number of lines for constant c_s and c .

Therefore, instead of completing these graphs with negative values of c_s and c and computing an analogous graph for c_a , it was decided to develop nomograms for c_s , c_a and c .

Several systems of nomograms would be required for c_s , c_a and c each, when basing them upon (1), (2) and (3). Though it would represent the exact solution, errors would be inevitable due to the complexity of the procedure. Therefore it seemed preferable to derive the nomograms from approximate formulae, offering the possibility to read the coefficients of restraint from one single nomogram. Likewise the graphs of ref. 4a and b have been derived from approximate solutions obtained by applying the energy-method.

The approximate solutions have been computed assuming for the

deflection of the plate

$$w = [A f_1(y) + B f_2(y)] \sin \frac{\pi x}{l},$$

where $f_1(y)$ and $f_2(y)$ satisfy the geometrical boundary conditions, and the ratio A/B is such that the dynamic boundary conditions at the rigidly supported edge(s) are satisfied.

The assumed deflections are

$$w_s = A \left\{ \cos \pi \frac{y}{b} + \frac{\pi c_s}{4(c_s+2)} \left[\left(\frac{2y}{b} \right)^2 - 1 \right] \right\} \sin \frac{\pi x}{l} \quad (6-4)$$

$$w_a = A \left\{ \sin 2\pi \frac{y}{b} + \frac{\pi c_a}{2(c_a+6)} \left[\left(\frac{2y}{b} \right)^2 - 1 \right] \frac{2y}{b} \right\} \sin \frac{\pi x}{l} \quad (6-5)$$

$$w = A \left\{ \frac{y}{b} - \frac{c}{19.556} \left[\left(\frac{y}{b} \right)^3 - 4.963 \left(\frac{y}{b} \right)^2 + 9.852 \left(\frac{y}{b} \right) - 9.778 \right] \left(\frac{y}{b} \right)^2 \right\} \sin \frac{\pi x}{l} \quad (6-6)$$

(4) and (6) have been taken from ref. 4a and b, since these assumptions yield a close approximation of k^2 ; (5) has been chosen in analogy to (4). In w_s , $f_2(y)$ represents the deflection of a beam, symmetrically loaded at its ends by bending moments in w_a , $f_1(y)$ is the deflection of a beam, antisymmetrically loaded at its ends by bending moments and corresponding shear loads. w_s and w_a satisfy the differential equation when $l \rightarrow \infty$ ($c_s = -2$, $c_a = -6$), and when $A/B \rightarrow \infty$ (simply supported edges)

The critical stress parameters k^2 calculated by applying the energy method, are:

for symmetrical buckling of a web

$$\pi^2 k^2 - \lambda^2 = \frac{\frac{\pi^2}{\lambda^2} \left[\left(\frac{1}{8} - \frac{1}{\pi^2} \right) c_s^2 + \left(\frac{1}{2} - \frac{2}{\pi^2} \right) c_s + \frac{1}{2} \right] + \left(\frac{5}{12} - \frac{4}{\pi^2} \right) c_s^2 + \left(1 - \frac{8}{\pi^2} \right) c_s + 1}{\left(\frac{\pi^2}{120} + \frac{1}{8} - \frac{2}{\pi^2} \right) c_s^2 + \left(\frac{1}{2} - \frac{4}{\pi^2} \right) c_s + \frac{1}{2}} \quad (6-7)$$

for anti-symmetrical buckling of a web

$$\pi^2 k^2 - \lambda^2 = \frac{\frac{\pi^2}{\lambda^2} \left[4 \left(1 - \frac{6}{\pi^2} \right) c_a^2 + 48 \left(1 - \frac{3}{\pi^2} \right) c_a + 144 \right] + \left(\frac{14}{5} - \frac{24}{\pi^2} \right) c_a^2 + 24 \left(1 - \frac{6}{\pi^2} \right) c_a + 72}{\left(\frac{\pi^2}{105} + \frac{1}{4} - \frac{3}{\pi^2} \right) c_a^2 + 6 \left(\frac{1}{2} - \frac{2}{\pi^2} \right) c_a + 9} \quad (6-8)$$

for a flange

$$\pi^2 k^2 - \lambda^2 = \frac{\frac{\pi^2}{\lambda^2} \left[0.14178 C^2 + C \right] + (0.08782 - 0.09868 \mu) C^2 + (0.79546 - 0.89395 \mu) C + 2(1 - \mu)}{0.010715 C^2 + 0.11847 C + 0.33333} \quad (6-9)$$

These results are of the general form:

$$\pi^2 k^2 - \lambda^2 = \frac{\pi^2}{\lambda^2} F(\zeta) + G(\zeta),$$

enabling the construction of nomograms for C with straight basic lines for $\pi^2 k^2 - \lambda^2$ and π/λ^2 . These nomograms have been given in figs. 8 and 9, where μ has been assumed to be $\mu = 0,3$.

6.2 The accuracy of the approximate solution.

In ref. 4 a and b a comparison is given of the approximate and the exact solutions. For $c_s \geq 0$ the error of k^2 is maximal 1% when $k^2 < 9$, and $l/b > 0,4$. For a flange with positive restraint the error of k^2 varies from 1/2% at $l/b = 10$ tot 2 1/2% at $l/b = 0,8$.

For negative c_s , c_a and c a comparison between the exact value and the approximate value, obtained from the nomograms, is given in table I, II and III resp.

Table I c_s according to a/ exact b/ approximate solution.

l/b k	0,6		0,7		0,8		0,9		1,2	
	a	b	a	b	a	b	a	b	a	b
0,7	-9,71	-	-7,96	-	-6,68	-	-5,72	-5,9	-4,04	-4,06
1,4	-8,44	-	-6,47	-	-5,09	-5,36	-4,16	-4,22	-2,80	-2,81
2,1	-3,19	-3,85	-0,581	-0,60	+0,856	+0,85	+1,229	+1,21	+0,493	+0,50
	2,0		6,0		∞					
0,7	-2,68	-2,68	-2,07	-2,07	-2	-2				
1,4	-2,13	-2,12	-2,00	-2,00	-2	-2				
2,1	-1,03	-1,03	-1,89	-1,89	-2	-2				

Table II c_a according to a/exact b/approximate solution.

l/b k	0,6		0,7		0,8		0,9		1,2	
	a	b	a	b	a	b	a	b	a	b
0,7	-10,83	-	-9,64	-10,1	-8,82	-9,00	-8,25	-8,32	-7,28	-7,28
1,4	-10,39	-	-9,26	-9,65	-8,48	-8,60	-7,95	-8,00	-7,08	-7,10
2,1	-9,55	-10,2	-8,50	-8,72	-7,84	-7,85	-7,41	-7,45	-6,74	-6,75
	2,0		6,0		∞					
0,7	-6,46	-6,46	-6,05	-6,05	-6	-6				
1,4	-6,38	-6,38	-6,04	-6,04	-6	-6				
2,1	-6,25	-6,25	-6,03	-6,03	-6	-6				

Table III c according to a/exact b/approximate solution

k \ l/b	1,5		2,0		2,5		3		4	
	a	b	a	b	a	b	a	b	a	b
0,3	-3,64	-3,66	-2,35	-2,41	-1,61	-1,66	-1,15	-1,17	-0,666	-0,67
0,7	-2,57	-2,61	-1,05	-1,08	-0,403	-0,40	-0,144	-0,14	> 0	
6		12								
	a	b	a	b						
	-0,300	-0,30	-0,101	-0,10						
	> 0		> 0							

Assuming the admissible error of c to be 5%, the nomograms can be used in the ranges of negative restraint:

$$c_s > -5, \frac{l}{b} > 0,7 ; c_a > -10, \frac{l}{b} > 0,7 ; c > -3, \frac{l}{b} > 1,5$$

A comparison of the results obtained from a calculation based upon the application of the nomograms and results available in literature is possible for U- and Z-sections with equal flanges and constant wall thickness (see table IV).

Table IV: k^2 (referring to web) for channel and Z-sections stringers (a = with of web, b = with of flange)

b/a	0,2	0,3	0,375	0,5	0,75	1,0
nomogram method	4,57	4,36	3,96	2,91	1,50	0,89
ref.5 approximate solution	4,59	4,39	3,96	2,92	1,50	0,89
ref.2 exact solution	-	-	4,00	2,907	1,496	0,885

The nomogram method and ref.5 have been based upon the same approximations for the deflections; so the results should be identical; the existing deviations give an impression of the reliability of the nomograms. Comparison with the exact solutions shows that the approximation is very close indeed; this comparison covers roughly the ranges of c_s and c.

$$0,375 \leq \frac{b}{a} \leq 1 \quad 0 > c_s > -2,50 ; \quad 0 < c < 2,70$$

Therefore a general conclusion on the accuracy of the approximative solution cannot be drawn. However it seems probable that the approximation cannot be in error for more than a few percents, since:

1. for positive coefficients of restraint the error of k^2 does not exceed 1 and $2\frac{1}{2}$ % for web and flanges resp.;
2. the important errors of the coefficients of restraint occur with small k and small l/b (see table I, II, III), whereas small k means narrow width of plate and small l/b means large width of plate; therefore it is unlikely that the region of large errors will be encountered in practice.

7. Applications

For all n walls of the composed cross section the coefficients of restraint, c_s and c_a for webs and C for flanges, are determined from the nomograms figs 8 and 9 after computing l/b and $k^2 = (b/l)^2$, where

$k^2 = \frac{2(1-\mu^2)}{\pi^2} \frac{\sigma}{E} \left(\frac{b}{t}\right)^2$. σ and l are equal for all walls. The computation is to be executed for 3 or 4 values of σ at 3 or 4 values of l . A guide for making a guess at l can be obtained from the consideration, that l will be smaller than the width of the largest web and larger than the width of the smallest web. A guess at σ can be obtained from the consideration that the web with largest b/t will obtain much restraint from the adjacent walls. Therefore the upper limit of σ will be that of a rigidly restrained plate with (see 6.7)

$$k^2 \approx 5.1 \left(\frac{l}{b}\right)^2 + 2.5 + (b/l)^2 \quad (7-1)$$

where b is the width of the web with largest b/t and l is the assumed half wave length.

Having determined the coefficients of restraint c the quantities

$S_i = \left(\frac{B}{b}\right)_i C_i$ are computed or $s_i = \left(\frac{b}{B}\right)_i \cdot \left(\frac{B}{b}\right)_i C_i$ where $\left(\frac{B}{b}\right)_i$ is an arbitrary unit of spring stiffness.

The computation ends with the determination of the required additional spring stiffness $R_{n-1,n}$. The general procedure to obtain R has been outlined in section 4.

In the following explicit formulae for R or $r = R \left(\frac{b}{B}\right)_i$ have been given, applying to $n \leq 5$, where the first and the last wall are flanges.

$$n=2: \quad r_{12} = S_1 + S_2 \quad (7-2)$$

$$n=3: \quad r_{23} = S_3 + \frac{2 S_{a2} S_{s2} + S_1 (S_{a2} + S_{s2})}{2 S_1 + S_{a2} + S_{s2}} \quad (7-3)$$

$$n=4: \quad r_{34} = S_4 + \frac{2 S_{a3} S_{s3} (2 S_1 + S_{a2} + S_{s2}) + [S_1 (S_{a2} + S_{s2}) + 2 S_{a2} S_{s2}] (S_{a3} + S_{s3})}{2 [S_1 (S_{a2} + S_{s2}) + 2 S_{a2} S_{s2}] + (2 S_1 + S_{a2} + S_{s2}) (S_{a3} + S_{s3})} \quad (7-4)$$

$$\begin{aligned}
 n=5: \quad r_{45} = & S_5 + \{ 2(2S_1 + S_{a2} + S_{s2})[S_{a3}S_{s3}(S_{a4} + S_{s4}) + S_{a4}S_{s4}(S_{a3} + S_{s3})] + \\
 & + [S_1(S_{a2} + S_{s2}) + 2S_{a2}S_{s2}][4S_{a4}S_{s4} + (S_{a3} + S_{s3})(S_{a4} + S_{s4})] \} : \\
 & \{ (2S_1 + S_{a2} + S_{s2})[4S_{a3}S_{s3} + (S_{a3} + S_{s3})(S_{a4} + S_{s4})] + \\
 & + 2[S_1(S_{a2} + S_{s2}) + 2S_{a2}S_{s2}](S_{a3} + S_{s3} + S_{a4} + S_{s4}) \} \quad (7-5)
 \end{aligned}$$

Formulae for more complicated sections, where $n \leq 5$ can be derived from (2) to (5). Some important cases have been considered in table V.

Table V Derived structures with $n \leq 5$

n	r given by formula	basic case	derived structures	replace	by
2	7-2		channel and Z-sections with equal flanges	S_2	S_{s2}
3	7-3		panel with Z-sections at equal intervals	S_3	$S_2' + 2S_{s3}$
			square tophat sections	S_3	S_{s3}
			panel with tophat sections at equal intervals	S_1 S_3	$S_{s1} + S_1'' + S_{s1}'$ S_{s3}
5	7-5		panel with alternating equal flanged Z-sections at equal intervals.	S_{a2} S_{s2} S_{a3} S_{s3} S_{a4} S_{s4}	$S_{a2} + S_2'$ $S_{s2} + S_2'$ $2S_{a3}$ $2S_{s3}$ $S_{a4} + S_3'''$ $S_{s4} + S_3'''$

8. Numerical example

The dimensions of a panel with alternating Z-stiffeners at equal distances. (fig.6) has dimensions as given in table VI.

Table VI. Basic data for numerical example

wall	t	b	b/t	$k_1^2/k_2^2 = (b/t)_1^2 : (b/t)_2^2$	$(B/b)_1 : (B/b)_2$	$(l/b)_1 : (l/b)_2$
1	4	30	7,5	0,160	2,5	2,5
2	4	75	18,75	1	1	1
2'	4	30	7,5	0,160	2,5	2,5
3	3	101	33,67	3,2240	0,3133	0,7426
3'''	3	20	6,67	0,1264	1,5820	3,75
4	3	50	16,67	0,7901	0,6328	1,50
5	3	20	6,67	0,1264	1,5820	3,75

The critical half wave length will be between b_3 and b_4 . The smaller Z-section will be of secondary importance for the wave length, so it may be expected that l is much larger than $b_4 = 50$. When wall 3 would be

rigidly restrained $\lambda = 0,660 \times 101 = 67$. With finite stiffness of restraint λ will exceed 67, but will not reach 101. Therefore practical limits for λ will be 75 and 90. Computations have been executed for λ : 75; 82,5 and 90 or $\frac{\lambda}{b^2} = 1,0; 1,1; 1,2$. Applying (7.1) the upper limits of k_3^2 will be 7.14; 7.41; 7.81. The lower limit is, neglecting edge restraint, $k_3^2 = 4$. Computations have been executed for k_3^2 : 4,51; 5,16; 5,80; 6,45 or $k_2^2 = 1,40; 1,60; 1,80$ and 2,00. In table VII the coefficients of restraint, read from fig.8 and 9, have been tabulated. The graphical representation of the coefficient of additional restraint r_4 , computed from (7,5) and given in fig.10 shows that the considered range of σ includes asymptotic values of r . This fact thwarts the graphical interpolation. This inconvenience can be overcome by determining the asymptote from $\Phi_{n-1,n} = 0$, again by graphical interpolation of $\Phi_{n-1,n}$.

Finally the interpolation of K_b^2 and K_{crit}^2 has been given in fig.10, yielding $K_{crit}^2 = 1,585$, $\frac{b}{b} = 1,2$. Assuming $E = 7 \cdot 10^5 \text{ kg/cm}^2$, $\sigma_{crit} = 2850 \text{ kg/cm}^2$. Comparison of table VII and tables I, II, III shows that the errors of c_a , c_s and c are very small indeed.

9. Notations

- a.: suffix, referring to anti-symmetrical deformation of plate, elastically restrained at both edges (web).
- b : width of a plate, web or flange
- c : coefficient of restraint of a flange
- c_a : " " " " " web, antisymmetrically distorted
- c_s : coefficient of restraint of a web, symmetrically distorted
- i : suffix for an arbitrary plate
- k : non-dimensional buckling coefficient, defined by
- λ : half wave length of buckling mode
- $m_{n-1,n}$: external moment required for equilibrium at joint $n-1,n$
- n : number of walls in the sequence i.
- 0 : suffix, referring to an arbitrarily chosen reference wall
- r : coefficient of additional restraint, defined by
- s : coefficient of restraint
- s : suffix referring to symmetrical deformation of plate, elastically restrained at both edges (web).

t : plate thickness
 w : deflection of plate
 x : longitudinal coordinate
 y : lateral coordinate of a plate
 B : plate stiffness =
 E : Young's modul
 $M_{i,j}$: edge moment in wall i at the joint with wall j , positive in anti-clockwise direction
 $R_{n-1,n}$: additional stiffness required for equilibrium = $-\left(\frac{m}{\phi}\right)_{n-1,n}$
 S : stiffness of restraint = $\frac{B}{b} C$
 $\phi_{i-1,i}$: rotation of wall i at the joint with wall j , positive in anti-clockwise direction
 λ : wave length parameter = $\pi \frac{b}{l}$
 μ : Poisson's ratio
 σ : compressive stress
 σ_b : buckling stress at half wave length l
 σ_{crit} : critical stress.

10. References

1. E.F.Bruhn: Analysis and design of airplane structures. Chapter B 5.
2. G.Kimm: Beitrag zur Stabilität dünnwandiger U-profile mit konstanter Wandstärke im Elastischen Bereich. Lufo Bd 18 S. 155/168.
3. W.S.Hemp and K.H.Griffin: The buckling in compression of panels with square top-hat stringers, The College of Aeronautics, Cranfield, Rep. no. 29.
4. a. E.E.Lundquist and E.Z.Stowell: Critical compressive stress for flat rectangular plate supported along all edges and elastically restrained against rotation along the unloaded edges. NACA rep. no. 733.
 b. E.E.Lundquist and E.Z.Stowell: Critical compressive stress for outstanding flanges, NACA rep. no. 734.
5. E.E.Lundquist and E.Z.Stowell: Local instability of columns with I, Z-channel and rectangular tube sections. NACA rep. no. 743.

Acknowledgements

The author wishes to express his appreciation to the "Delfts Hogeschoolfond" for supplying the funds enabling him to complete this investigation, and to Ir J.L.Overbeeke, who developed the nomograms and made the calculations.

August 1952

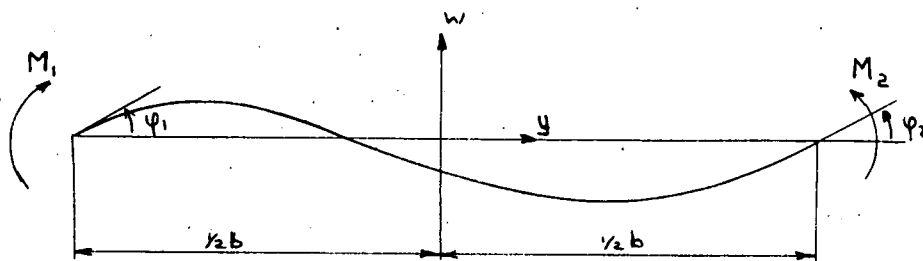


fig.1 Buckling mode of a plate with edge restraint

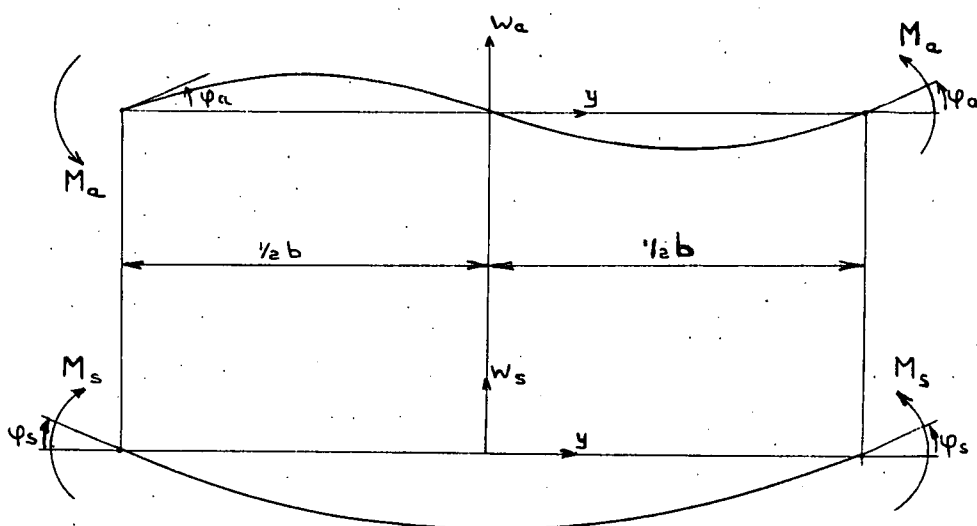


fig.2 Decomposition of buckling mode into a symmetrical and an anti-symmetrical part.

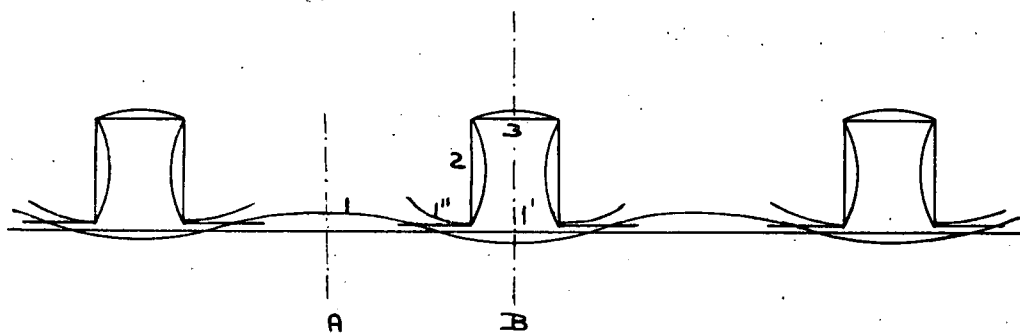


fig. 5 Critical mode of panel with regularly spaced tophat section stiffeners

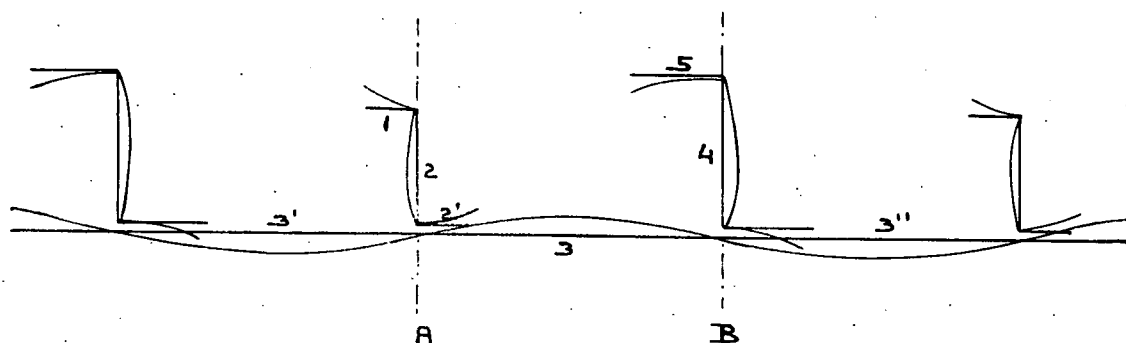


fig. 6 Critical mode of panel with regularly spaced Z-stiffeners of alternating size..

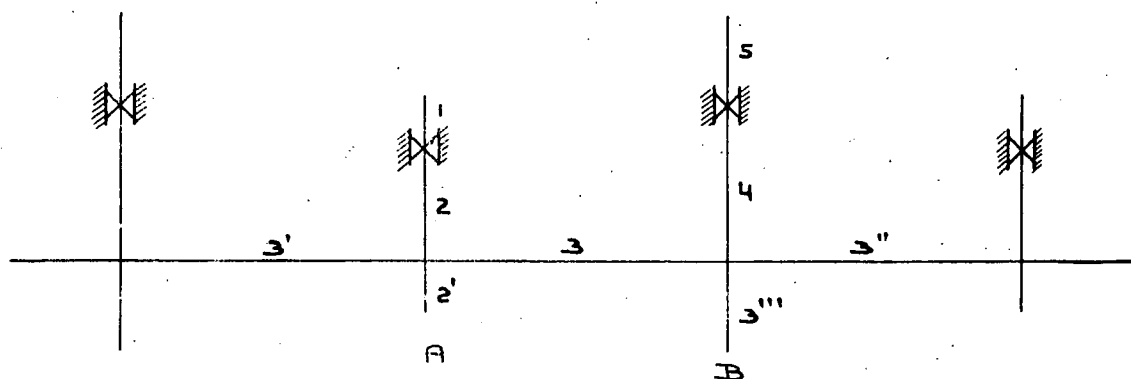


fig. 7 Structure equivalent to that of fig. 6

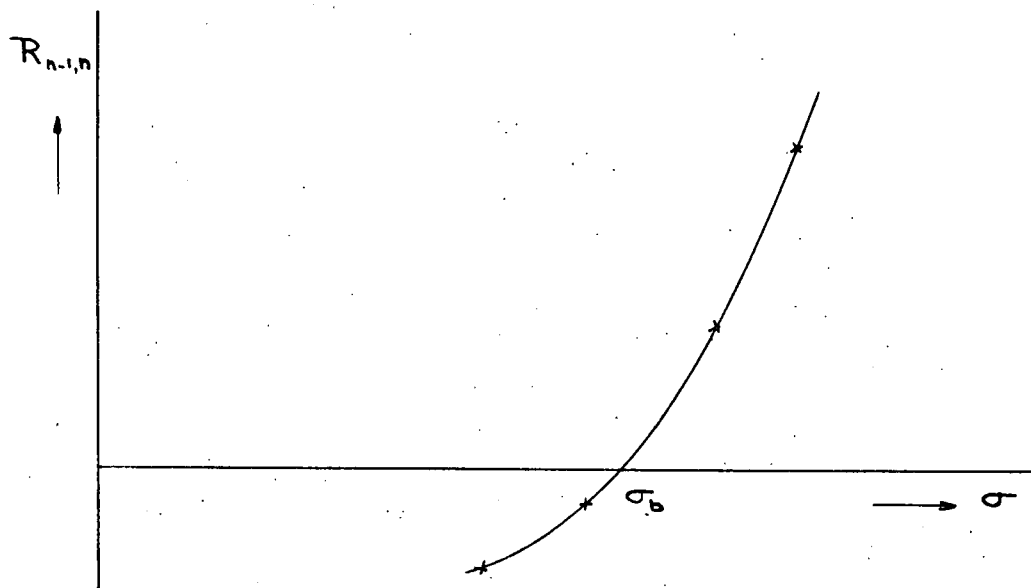


fig.3 Graphical determination of σ_b

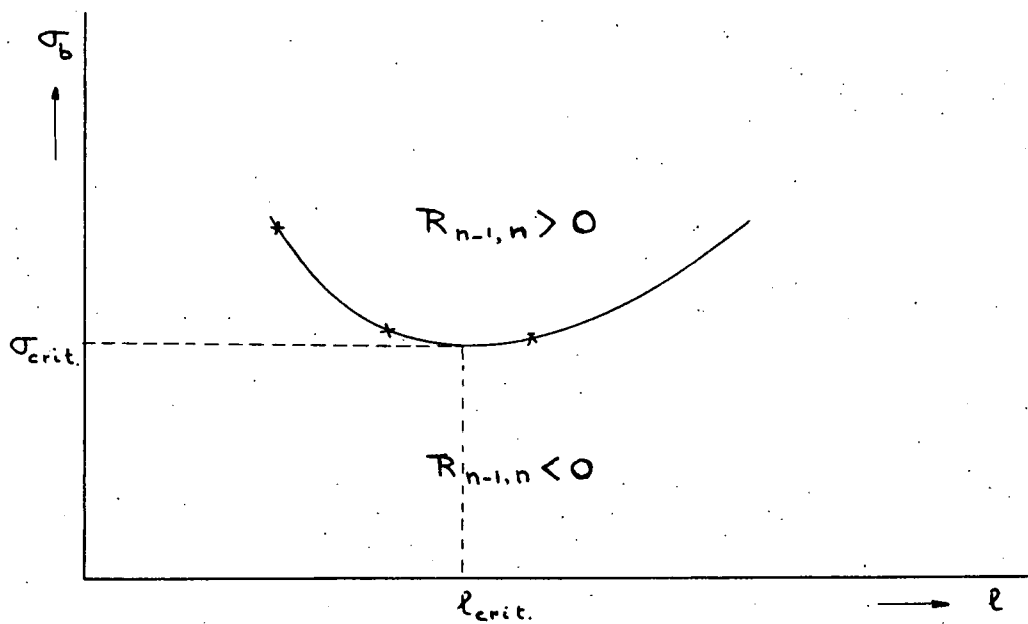


fig.4 Graphical determination of σ_{crit}

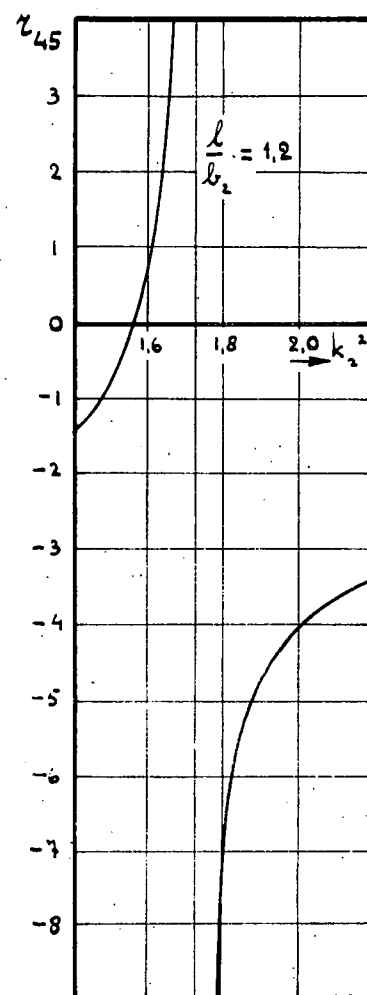
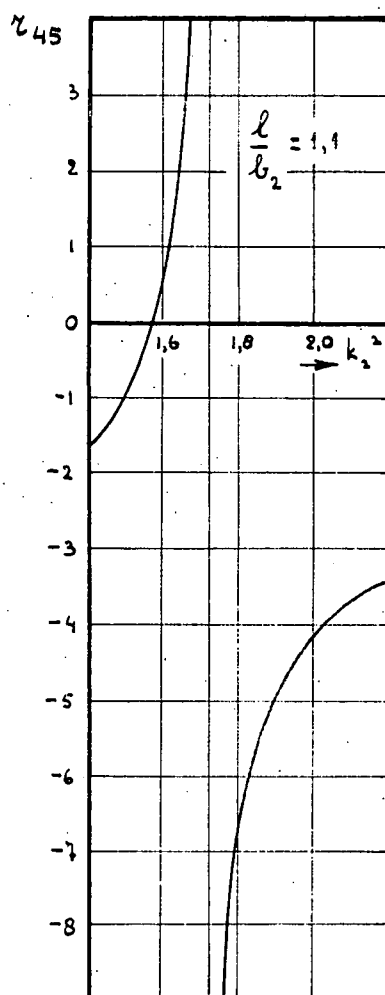
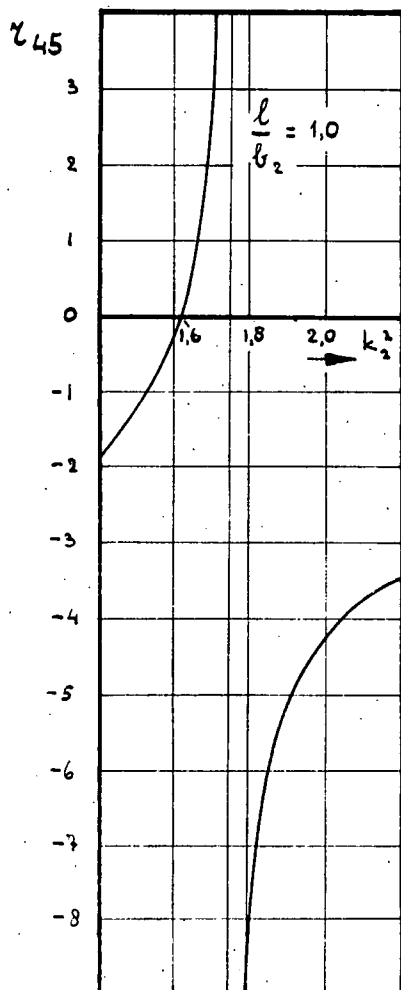


Fig. 10 Grafical interpolation of k_{2b}^2 and k_{2crit}^2 .

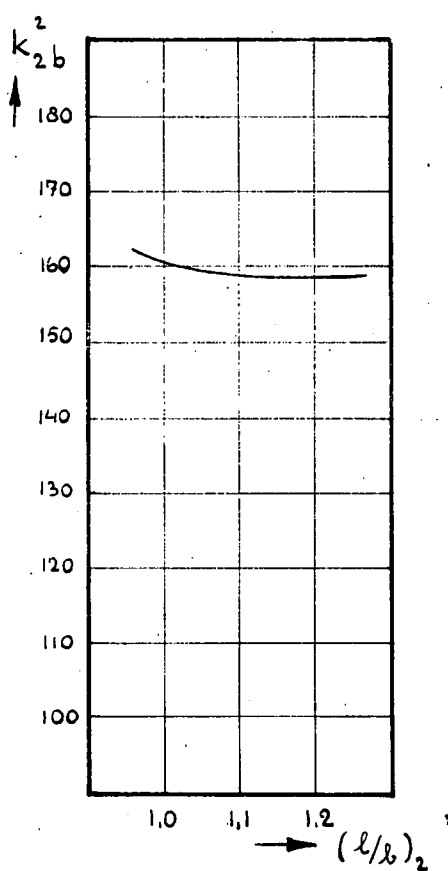


Table VII Numerical Example: Coefficients of restraint and results

i	1 and 2'				2							
l	l/b	k ²	k ² -(b/l) ²	ϕ	l/b	k ²	k ² -(b/l) ²	C _a	C _s			
75	2,50	0.224	0.064	-1.30	1.00	1.40	-0.40	-7.70	-4.21			
		0.256	0.096	-1.22		1.60	0.60	-7.66	-3.98			
		0.288	0.128	-1.13		1.80	0.80	-7.62	-3.76			
		0.320	0.160	-1.03		2.00	1.00	-7.58	-3.52			
82.5	2.75	0.224	0.092	-1.07	1.10	1.40	0.57	-7.40	-3.70			
		0.256	0.124	-0.99		1.60	0.77	-7.37	-3.50			
		0.288	0.156	-0.90		1.80	0.97	-7.34	-3.30			
		0.320	0.188	-0.81		2.00	1.17	-7.30	-3.07			
90	3.00	0.224	0.113	-0.88	1.20	1.40	0.71	-7.17	-3.34			
		0.256	0.145	-0.80		1.60	0.91	-7.14	-3.16			
		0.288	0.177	-0.72		1.80	1.11	-7.12	-2.97			
		0.320	0.209	-0.64		2.00	1.31	-7.09	-2.78			
3					4							
l/b	k ²	k ² -(b/l) ²	C _a	C _s	l/b	k ²	k ² -(b/l) ²	C _a	C _s			
0.743	4.51	2.70	-8.16	+0.71	1.50	1.11	0.66	-6.77	-2.92			
	5.16	3.35	-8.04	4.65		1.26	0.82	-6.75	-2.81			
	5.80	3.99	-7.82	12.6		1.42	0.98	-6.74	-2.72			
	6.45	4.64	-7.58	35		1.58	1.14	-6.72	-2.61			
0.817	4.51	3.01	-7.80	+1.40	1.65	1.11	0.74	-6.63	-2.72			
	5.16	3.66	-7.60	5.00		1.26	0.90	-6.62	-2.64			
	5.80	4.30	-7.42	11.7		1.42	1.05	-6.61	-2.56			
	6.45	4.95	-7.22	26.5		1.58	1.21	-6.59	-2.47			
0.891	4.51	3.25	-7.45	+1.60	1.80	1.11	0.80	-6.53	-2.59			
	5.16	3.90	-7.29	4.70		1.26	0.95	-6.52	-2.51			
	5.80	4.54	-7.11	9.9		1.42	1.11	-6.51	-2.44			
	6.45	5.19	-6.95	20		1.58	1.27	-6.50	-2.37			
3''' and 5												
l/b	k ²	k ² -(b/l) ²	C		r ₄₅	k ² _{2b}	k ² _{2crit}	(l/b) ₂ kr				
3.75	0.177	0.106	-0.62		-1.97	1.60 ⁵	1.58 ⁵					
	0.202	0.131	-0.58		-0.23							
	0.228	0.157	-0.53		-8.19							
	0.253	0.182	-0.48		-4.17							
4.125	0.177	0.118	-0.51		-1.67	1.59		1.58 ⁵	1.2			
	0.202	0.143	-0.47		+0.55							
	0.228	0.169	-0.42		-6.54							
	0.253	0.194	-0.39		-4.03							
4.50	0.177	0.128	-0.41		-1.49	1.58 ⁵			1.58 ⁵			
	0.202	0.153	-0.38		+0.63							
	0.228	0.179	-0.34		-7.44							
	0.253	0.204	-0.31		-3.99							
TECHNISCHE HOGESCHOOL					RAPPORT							
VLIETUIGBOUWKUNDE					47							

